16. S. Yellin, *Phys. Rev. D Part. Fields* **66**, 032005 (2002).
17. J. R. Ellis, K. A. Olive, Y. Santoso, V. C. Spanos, *Phys. Rev. D Part. Fields Gravit. Cosmol.* **71**, 095007 (2005).
18. L. Roszkowski, R. Ruiz de Austri, R. Trotta, *J. High Energy Phys.* **2007**, 075 (2007).
19. J. Angle *et al.*, *Phys. Rev. D Part. Fields Gravit. Cosmol.* **80**, 115005 (2009).
20. The CDMS collaboration gratefully acknowledges the contributions of numerous engineers and technicians; we would like to especially thank J. Beaty, B. Hines, L. Novak, R. Schmitt, and A. Tomada. This work is supported in part by the National Science Foundation (grants AST-9978911, PHY-0542066, PHY-0503729, PHY-0503629, PHY-0503641, PHY-0504224, PHY-0705052, PHY-0801708, PHY-0801712, PHY-0802575, and PHY-0855525), by the Department of Energy (contracts DE-AC03-76SF00098, DE-FG02-91ER40688, DE-FG02-92ER40701, DE-FG03-90ER40569, and DE-FG03-91ER40618), by the Swiss National Foundation (SNF grant 20-118119), and by the Natural Sciences and Engineering Research Council of Canada (grant SAPIN 341314-07).

The CDMS II Collaboration

Z. Ahmed,[1] D. S. Akerib,[2] S. Arrenberg,[18] C. N. Bailey,[2] D. Balakishiyeva,[16] L. Baudis,[18] D. A. Bauer,[3] P. L. Brink,[10] T. Bruch,[18] R. Bunker,[14] B. Cabrera,[10] D. O. Caldwell,[14] J. Cooley,[9] P. Cushman,[17] M. Daal,[13] F. DeJongh,[3] M. R. Dragowsky,[2] L. Duong,[17] S. Fallows,[17] E. Figueroa-Feliciano,[5] J. Filippini,[1] M. Fritts,[17] S. R. Golwala,[1] D. R. Grant,[2] J. Hall,[3] R. Hennings-Yeomans,[2] S. A. Hertel,[5] D. Holmgren,[3] L. Hsu,[3] M. E. Huber,[15] O. Kamaev,[17] M. Kiveni,[11] M. Kos,[11] S. W. Leman,[5] R. Mahapatra,[12] V. Mandic,[17] K. A. McCarthy,[5] N. Mirabolfathi,[13] D. Moore,[1] H. Nelson,[14] R. W. Ogburn,[10] A. Phipps,[13] M. Pyle,[10] X. Qiu,[17] E. Ramberg,[3] W. Rau,[6] A. Reisetter,[17,7] T. Saab,[16] B. Sadoulet,[4,13] J. Sander,[14] R. W. Schnee,[11] D. N. Seitz,[13] B. Serfass,[13] K. M. Sundqvist,[13] M. Tarka,[18] P. Wikus,[5] S. Yellin,[10,14] J. Yoo,[3] B. A. Young,[8] J. Zhang[17]

[1]Division of Physics, Mathematics and Astronomy, California Institute of Technology, Pasadena, CA 91125, USA. [2]Department of Physics, Case Western Reserve University, Cleveland, OH 44106, USA. [3]Fermi National Accelerator Laboratory, Batavia, IL 60510, USA. [4]Lawrence Berkeley National Laboratory, Berkeley, CA 94720, USA. [5]Department of Physics, Massachusetts Institute of Technology, Cambridge, MA 02139, USA. [6]Department of Physics, Queen's University, Kingston, ON K7L 3N6, Canada. [7]Department of Physics, St. Olaf College, Northfield, MN 55057, USA. [8]Department of Physics, Santa Clara University, Santa Clara, CA 95053, USA. [9]Department of Physics, Southern Methodist University, Dallas, TX 75275, USA. [10]Department of Physics, Stanford University, Stanford, CA 94305, USA. [11]Department of Physics, Syracuse University, Syracuse, NY 13244, USA. [12]Department of Physics, Texas A&M University, College Station, TX 77843, USA. [13]Department of Physics, University of California, Berkeley, CA 94720, USA. [14]Department of Physics, University of California, Santa Barbara, CA 93106, USA. [15]Departments of Physics and Electrical Engineering, University of Colorado Denver, Denver, CO 80217, USA. [16]Department of Physics, University of Florida, Gainesville, FL 32611, USA. [17]School of Physics and Astronomy, University of Minnesota, Minneapolis, MN 55455, USA. [18]Physics Institute, University of Zürich, Winterthurerstrasse 190, CH-8057, Switzerland.

Supporting Online Material
www.sciencemag.org/cgi/content/full/science.1186112/DC1
SOM Text
Figs. S1 to S4
References

17 December 2009; accepted 5 February 2010
Published online 11 February 2010;
10.1126/science.1186112
Include this information when citing this paper.

Downloaded from http://science.sciencemag.org/ on March 28, 2019

Anomalous Expansion of Attractively Interacting Fermionic Atoms in an Optical Lattice

Lucia Hackermüller,[1] Ulrich Schneider,[1,2] Maria Moreno-Cardoner,[1,2] Takuya Kitagawa,[3] Thorsten Best,[1] Sebastian Will,[1,2] Eugene Demler,[3] Ehud Altman,[4] Immanuel Bloch,[1,2,5] Belén Paredes[1]*

The interplay of thermodynamics and quantum correlations can give rise to counterintuitive phenomena in many-body systems. We report on an isentropic effect in a spin mixture of attractively interacting fermionic atoms in an optical lattice. As we adiabatically increase the attraction between the atoms, we observe that the gas expands instead of contracting. This unexpected behavior demonstrates the crucial role of the lattice potential in the thermodynamics of the fermionic Hubbard model.

The striking consequences of correlations in many-body quantum systems are at the frontier of current research. Typically, interest is devoted to the unusual properties of ground states or low-lying excitations, such as exotic types of order and unconventional quasi-particle statistics (*1*, *2*). But correlations can also alter the thermodynamics of a quantum system, leading to fascinating finite-temperature effects. Especially surprising behavior can arise when the system adiabatically enters a strongly correlated phase, as the emerging correlations can imply a substantial redistribution of entropy. A well-known example is the Pomeranchuk effect (*3*, *4*), which occurs in the liquid-to-solid transition of ^{3}He. As a result of its randomly oriented spins, the solid is more disordered than the liquid. When adiabatically squeezed, the liquid therefore freezes into a solid by absorbing heat.

Recently, the extraordinary progress in the control and manipulation of neutral atoms in optical lattices (*5*–*7*) has added a valuable degree of freedom to the investigation of strongly correlated systems. By varying a collection of parameters such as scattering length, lattice depth, and external confinement, it is possible to adiabatically bring a weakly interacting gas of bosonic (*7*) or fermionic atoms (*8*–*11*) into a regime of strong correlations. The versatility of these systems makes them ideal candidates not only to simulate strongly correlated many-body phases, but also to investigate intriguing thermodynamic effects. In particular, the simulation and investigation of the single-band attractive fermionic Hubbard model has received special interest (*12*–*16*), both as a means of accessing the preformed-pair or pseudogap regime (*12*–*15*) and as an alternative route to study the physics of the repulsive Hubbard model (*16*), possibly providing insight into the origin of high-temperature superconductivity in cuprates (*17*, *18*).

We consider an attractively interacting spin mixture of fermionic atoms in two distinct hyperfine states loaded into the lowest band of a three-dimensional (3D) optical lattice and placed in an external harmonic potential. Its physics can be described by a Hubbard Hamiltonian with an additional harmonic confining term:

$$\hat{H} = -t \sum_{\langle \ell,\ell' \rangle \sigma} c^{\dagger}_{\ell\sigma} c_{\ell'\sigma} + U \sum_{\ell} \hat{n}_{\ell\uparrow} \hat{n}_{\ell\downarrow} + E_c \sum_{\ell\sigma} r_\ell^2 \hat{n}_{\ell\sigma} \qquad (1)$$

where $c_{\ell\sigma}$, $c^{\dagger}_{\ell\sigma}$, and $\hat{n}_{\ell\sigma}$ are, respectively, the fermionic annihilation operator, the fermionic creation operator, and the particle number operator at lattice site ℓ (with dimensionless coordinates x, y, and z), and spin state $\sigma \in \{\uparrow,\downarrow\}$, corresponding to the two hyperfine states. We consider the case of an unpolarized system with $N_\sigma = N/2$, where N_σ is the number of particles per spin component and N is the total number of particles. The Hamiltonian (Eq. 1) consists of three competing terms. The first term accounts for the kinetic energy of the system, which is characterized by the hopping amplitude t between neighboring lattice sites; the second term describes the attractive on-site interaction $U < 0$ between atoms with opposite spin (Fig. 1A). The last term represents the confinement energy due to the external anisotropic harmonic potential. The characteristic energy $E_c = V_c r_c^2$ is the mean potential energy per particle and spin state of a maximally packed state at the bottom of the trap, where $r_c^2 d^2$ is the corresponding mean squared radius, $V_c = {}^1/_2 m\omega_\perp^2 d^2$, $\omega_\perp = \omega_x = \omega_y = \omega_z/\gamma$ [where $\omega_{x,y}$ are the horizontal trap frequencies and ω_z is the vertical trap frequency], m is the mass of

[1]Institut für Physik, Johannes Gutenberg-Universität, 55099 Mainz, Germany. [2]Ludwig-Maximilians-Universität, 80799 München, Germany. [3]Department of Physics, Harvard University, Cambridge, MA 02138, USA. [4]Department of Condensed Matter Physics, Weizmann Institute of Science, Rehovot 76100, Israel. [5]Max-Planck-Institut für Quantenoptik, 85748 Garching, Germany.

*To whom correspondence should be addressed. E-mail: paredes@uni-mainz.de

an atom, and d is the lattice constant. The squared radius at site ℓ is $r_\ell^2 = (1/r_c^2)(x^2 + y^2 + \gamma^2 z^2)$.

We want to study the size behavior of the system when adiabatically entering the regime of dominating attractive interaction U. To characterize the size, we define the radius R according to

$$R^2 = \frac{1}{N_\sigma}\sum_\ell r_\ell^2 n_\ell \qquad (2)$$

where $n_\ell = \langle \hat{n}_{\ell\sigma} \rangle$, the brackets denoting the expectation value at finite temperature. With this definition, the average potential energy per particle and spin state is $E_c R^2$ and the radius of the maximally packed state is equal to 1. As a measure of the change in size in response to an adiabatic change of the interaction strength, we define the interaction compressibility

$$\kappa_i = \frac{\partial R^2}{\partial U}\bigg|_S \qquad (3)$$

in analogy to the volume compressibility $\kappa_c = -\partial R^2/\partial E_c|_S$ (*11*).

In the experiment, an equal mixture of quantum degenerate fermionic ^{40}K atoms in the two hyperfine states $|F, m_F\rangle = |{}^9/_2, -{}^9/_2\rangle \equiv |\downarrow\rangle$ and $|{}^9/_2, -{}^7/_2\rangle \equiv |\uparrow\rangle$ is used. By overlapping two orthogonally propagating laser beams with elliptical shape, a pancake-shaped dipole trap with an aspect ratio $\gamma \approx 4$ is formed. With the use of evaporative cooling in this trap, it is possible to reach temperatures down to $T/T_F = 0.12 \pm 0.03$ (where T_F is the Fermi temperature) with 1.4×10^5 to 1.8×10^5 atoms per spin state. The combination of a red-detuned dipole trap ($\lambda_{dip} = 1030$ nm) and a blue-detuned optical lattice ($\lambda_{lat} = 738$ nm) with simple cubic geometry allows an independent control of the confinement energy E_c and the tunneling t. By means of a Feshbach resonance located at 202.1 G (*19*), the on-site interaction energy U can be tuned at constant tunneling. Negative scattering lengths up to $a = -400 a_0$ can be reached; a further approach to the Feshbach resonance is hindered by enhanced losses, heating, and nonadiabatic effects in the lattice (*19*).

After evaporation, the dipole trap depth is ramped in 100 ms to the desired value of the external confinement ($\omega_\perp = 2\pi \times 20$ to 70 Hz) and the magnetic field is adjusted to set the scattering length. Subsequently, the optical lattice is increased to a potential depth $V_{lat} = 0$ to 9 E_r with a ramp rate of 7 ms/E_r (*19*), where $E_r = h^2/(2m\lambda_{lat}^2)$ is the recoil energy and h is the Planck constant.

We used phase-contrast imaging to extract the cloud size from in situ images taken along the short axis of the trap (*19*). The experimental data (Fig. 2A) show a contraction of the gas for weak attractive interactions followed by an anomalous expansion for interactions larger than a critical value, which typically corresponds to a scattering length $|a| \approx 20$ to 40 a_0. Additionally, the fraction of atoms sitting on doubly occupied sites (doublon fraction) is measured via conversion into molecules (*11*, *19*–*21*), showing a steep increase as the interaction becomes attractive (Fig. 2B). The number of doublons surprisingly continues to increase as the gas expands, saturating close to 80% for strong interactions and deep lattices. This high doublon fraction, at a density substantially lower than two atoms per site, indicates that the system is in a preformed-pair regime (*15*). In the absence of the lattice (Fig. 2A), we find that the anomalous expansion disappears [see also (*22*)] and the size of the cloud remains constant, whereas the doublon fraction can still increase to >40% when the free atom cloud is projected into the lattice.

The theoretical analysis of our results is simplest in the zero tunneling limit, where quantum fluctuations are completely suppressed. In this limit the Hamiltonian is a sum of local Hamiltonians at each site:

$$\hat{h}_\ell = U\hat{n}_{\ell\uparrow}\hat{n}_{\ell\downarrow} + E_c r_\ell^2(\hat{n}_{\ell\uparrow} + \hat{n}_{\ell\downarrow}) \qquad (4)$$

Hence, the problem factorizes into local on-site problems characterized by the probabilities for zero, single, and double site occupation, and the thermodynamic properties can be calculated exactly (*19*). As interaction increases from zero to infinitely attractive, single occupation is progressively suppressed and the system evolves from a gas of noninteracting fermions with spin, and local entropy $s_\ell = -2[n_\ell \log n_\ell + (1 - n_\ell)\log(1 - n_\ell)]$, to a system of on-site pairs (Fig. 1, B and C). In contrast to pairs in the continuum, which can Bose-condense in the same quantum state, these hard-core bosons occupy lattice sites according to Fermi statistics and have local entropy $s_\ell = -[n_\ell \log n_\ell + (1 - n_\ell)\log(1 - n_\ell)]$, as if they were fermions without spin. The progressive loss of the spin degree of freedom induced by pairing causes a continuous reduction of the entropy density (Fig. 3A). For the same radius (the same n_ℓ), the entropy that can be stored is exactly reduced by a factor of 2. At a fixed entropy, this reduction forces the system to

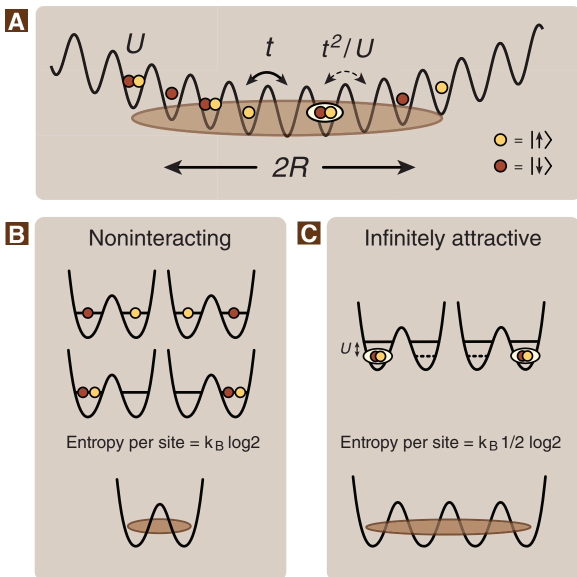

Fig. 1. Attractively interacting fermionic spin mixture in an optical lattice. (**A**) The system size R is determined by the interplay among entropy and the different energy scales: the interaction U, the tunneling amplitude t, and the confinement energy. For strong attractive interaction, on-site pairs are formed, which tunnel via second-order processes of amplitude t^2/U. (**B** and **C**) Schematic illustration of the anomalous expansion using a zero-tunneling two-particle model. The entropy that can be stored per site is reduced as the system evolves from the noninteracting regime, with four possible configurations (B), to the infinitely attractive regime, where particles are tightly bound and only two configurations are available (C). This reduction of entropy per site causes the system to expand [(B) and (C), bottom].

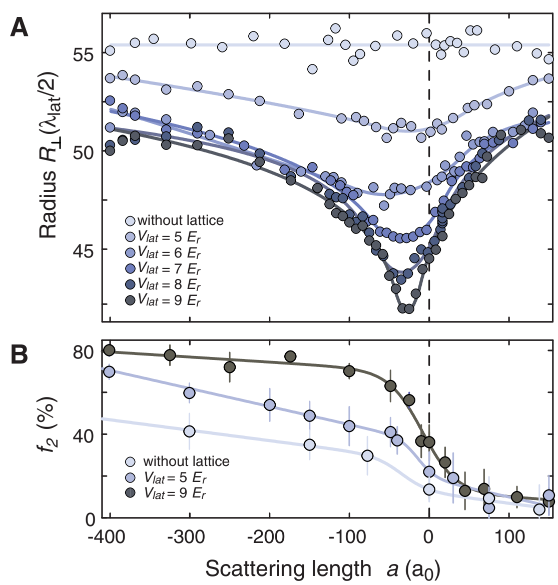

Fig. 2. Experimental observation of anomalous expansion. (**A**) Measured cloud size $R_\perp$ and (**B**) fraction of particles on doubly occupied sites f_2 (doublon fraction) versus scattering length for different lattice depths (5 and 9 E_r) and in the absence of the lattice. Solid circles in (A) correspond to a running average over three experimental shots. Solid circles in (B) are averages over at least five consecutive measurements, with the standard deviation plotted as the error bar. Lines are guides to the eye. Data were taken in a fixed external dipole trap with $\omega_\perp = 2\pi \times 25$ Hz and aspect ratio $\gamma \approx 4$, at a fixed temperature (before loading of the lattice) of $T/T_F = 0.15 \pm 0.03$ (*19*).

Downloaded from http://science.sciencemag.org/ on March 28, 2019

expand as the attraction increases, exhibiting a negative interaction compressibility κ_i for any nonvanishing attraction and entropy (Fig. 3C).

At finite tunneling, energy minimization and reduction of entropy density compete for the sign of κ_i. For weak attractive interaction, the behavior of the radius is expected to be dominated by the zero-entropy radius, and the system is expected to exhibit a positive κ_i. For a sufficiently strong attractive interaction, however, the system turns into a gas of hard-core pairs, whose kinetic energy t^2/U vanishes with increasing attraction. The influence of energy then becomes negligible and the reduction of entropy density should dominate, with the system increasing its size and exhibiting a negative κ_i. The value of attractive interaction above which the compressibility becomes negative should increase with tunneling. As tunneling increases, the role of interactions is effectively diminished and a larger interaction is required for the entropic effect to overcome the energy minimization effect. The above predictions can be illustrated by exact diagonalization of a small system (*19*) (figs. S1 and S2). The full many-body problem cannot be solved exactly because of the strong correlations involved. To analyze a 3D many-particle system, we use a high-temperature approximation (*19*, *23*–*25*) that treats interaction exactly and applies when tunneling is much smaller than either interaction or temperature. The first two terms of the high-temperature expansion capture the competition between energy and entropy and predict a minimum in the cloud radius (Fig. 4D).

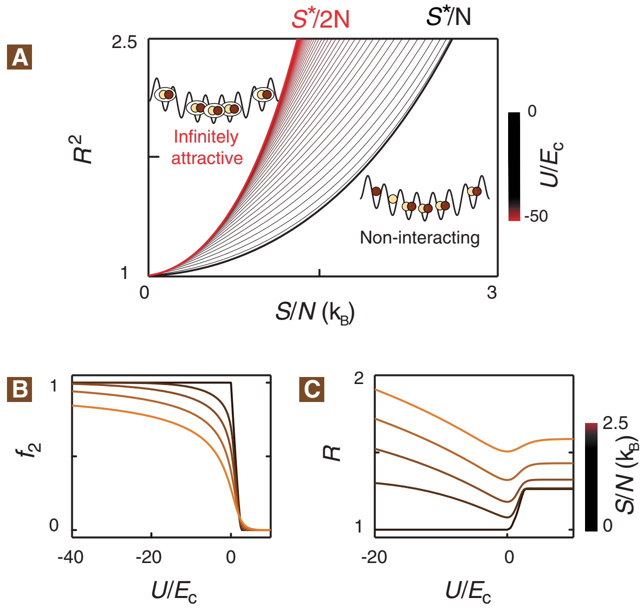

Fig. 3. Origin of negative compressibility at zero tunneling. Numerical exact calculation at zero tunneling for a 3D system with $N_\sigma = 7.5 \times 10^3$. (**A**) The squared radius R^2 plotted versus entropy per particle S/N for different attractive interaction strengths, ranging from $U = 0$ (black curve) to $U = -\infty$ (red curve). For a fixed nonvanishing entropy, the radius increases as the attraction increases. At fixed radius, the entropy for the noninteracting gas S^*/N is twice that for the infinite-attraction case. (**B**) Fraction of particles on doubly occupied sites (doublons) and (**C**) radius versus interaction strength at different fixed entropies.

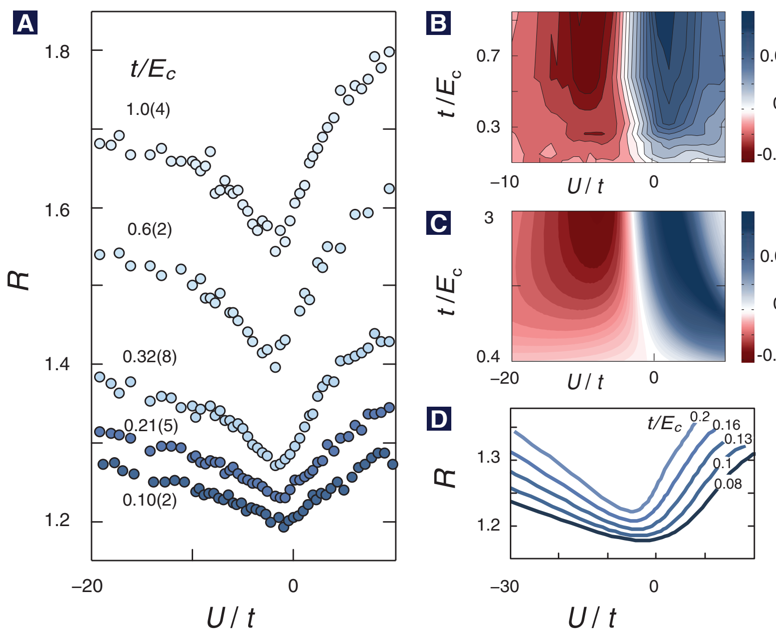

Fig. 4. Comparison of experimental and theoretical size behavior. (**A**) Measured rescaled radius R versus interaction strength U/t for different external confinements t/E_c. Lattice depth is fixed at $7E_r$, and entropy is $S/(k_BN)$ = 0.9 to 1.4 ($T/T_F = 0.12 \pm 0.03$). The radius is rescaled in units of the radius of a maximally packed system (see text). (**B** and **C**) Experimental (B) and calculated (C) compressibility κ_i via exact diagonalization of a small system at $S/(k_BN) = 0.7$ (*19*). Experimental compressibilities are determined from the measured cloud size via a linear fit to 10 consecutive data points. (**D**) Calculated radius of an atom cloud in a 3D lattice using a high-temperature expansion for different external confinements at fixed entropy $S/(k_BN) = 1.6$.

In Fig. 4A we show the experimental data obtained at fixed lattice depth for different external confinements, for which the ratios U/t and t/E_c are varied independently. The experimental observation and the theoretical prediction show the same qualitative features (Fig. 4, B and C). For increasing tunneling (decreasing confinement), the observed transition from positive to negative compressibility shifts to stronger attractive interactions. Note that for large ratios of t/E_c, where the role of the external confinement becomes unimportant, the transition occurs at a nearly constant value of U/t—the only energy scale left in the problem.

The size expansion of the gas observed in the experiment when increasing the interaction from zero to the maximum experimental negative value ($|U/t| \approx 20$) is on the order of 5 to 8%. To rule out a possible size increase due to heating, we measured temperatures after reversing the lattice-loading process for all scattering lengths (*19*). For large values of t/E_c, where the size increase is largest, a very small heating was observed (~1% of T_F), which could account for only a negligible expansion of the gas (up to ~1%), below the experimental shot-to-shot variation.

Our results show how pair formation in an attractively interacting spin mixture of fermionic atoms in an optical lattice gives rise to an anomalous expansion of the gas as the attraction increases. The consequences of pairing in the first band of a lattice potential are fundamentally different from the consequences of pairing in the continuum. Examples of exotic thermodynamic behavior caused by the interplay of strong interactions and entropy have been scarcely observed in quantum many-body systems. We anticipate that such effects can also occur for attractive Fermi mixtures with population imbalance (*26*), which are currently under investigation. Our work also opens an interesting route toward the detection of quantum many-body phases at finite entropies, where a marked change in the thermodynamic behavior can serve as a footprint of the crossover between two phases exhibiting substantially different entropy densities, as observed recently for a quantum critical system (*27*). This might be a promising perspective for the detection of transitions between two topological phases

Downloaded from http://science.sciencemag.org/ on March 28, 2019

(*28*), whose different topology can lead to strikingly distinctive ways of storing entropy (*29*).

References and Notes

1. A. Auerbach, *Interacting Electrons and Quantum Magnetism* (Springer, New York, 2006).
2. X. G. Wen, *Quantum Field Theory of Many-Body Systems* (Oxford Univ. Press, Oxford, 2004).
3. I. Pomeranchuk, *Zh. Eksp. Teor. Fiz.* **20**, 919 (1950).
4. R. C. Richardson, *Rev. Mod. Phys.* **69**, 683 (1997).
5. D. Jaksch, P. Zoller, *Ann. Phys.* **315**, 52 (2005).
6. M. Lewenstein *et al.*, *Adv. Phys.* **56**, 243 (2007).
7. I. Bloch, J. Dalibard, W. Zwerger, *Rev. Mod. Phys.* **80**, 885 (2008).
8. J. K. Chin *et al.*, *Nature* **443**, 961 (2006).
9. N. Strohmaier *et al.*, *Phys. Rev. Lett.* **99**, 220601 (2007).
10. R. Jördens, N. Strohmaier, K. Günter, H. Moritz, T. Esslinger, *Nature* **455**, 204 (2008).
11. U. Schneider *et al.*, *Science* **322**, 1520 (2008).
12. M. Randeria, N. Trivedi, A. Moreo, R. T. Scalettar, *Phys. Rev. Lett.* **69**, 2001 (1992).
13. A. Toschi, P. Barone, M. Capone, C. Castellani, *N. J. Phys.* **7**, 7 (2005).
14. C.-C. Chien, Q. Chen, K. Levin, *Phys. Rev. A* **78**, 043612 (2008).
15. T. Paiva, R. Scalettar, M. Randeria, N. Trivedi, http://arxiv.org/pdf/0906.2141 (2009).
16. A. F. Ho, M. A. Cazalilla, T. Giamarchi, *Phys. Rev. A* **79**, 033620 (2009).
17. P. Lee, N. Nagaosa, X.-G. Wen, *Rev. Mod. Phys.* **78**, 17 (2006).
18. W. Hofstetter, J. I. Cirac, P. Zoller, E. Demler, M. D. Lukin, *Phys. Rev. Lett.* **89**, 220407 (2002).
19. See supporting material on *Science* Online.
20. C. A. Regal, C. Ticknor, J. L. Bohn, D. S. Jin, *Nature* **424**, 47 (2003).
21. T. Stöferle, H. Moritz, K. Günter, M. Köhl, T. Esslinger, *Phys. Rev. Lett.* **96**, 030401 (2006).
22. M. Bartenstein *et al.*, *Phys. Rev. Lett.* **92**, 120401 (2004).
23. W. Metzner, *Phys. Rev. B* **43**, 8549 (1991).
24. J. A. Henderson, J. Oitmaa, M. C. B. Ashley, *Phys. Rev. B* **46**, 6328 (1992).
25. V. W. Scarola, L. Pollet, J. Oitmaa, M. Troyer, *Phys. Rev. Lett.* **102**, 135302 (2009).
26. S. Giorgini, L. Pitaevskii, S. Stringari, *Rev. Mod. Phys.* **80**, 1215 (2008).
27. A. W. Rost, R. S. Perry, J.-F. Mercure, A. P. Mackenzie, S. A. Grigera, *Science* **325**, 1360 (2009).
28. C. Nayak, S. H. Simon, A. Stern, M. Freedman, S. Das Sarma, *Rev. Mod. Phys.* **80**, 1083 (2008).
29. N. R. Cooper, A. Stern, *Phys. Rev. Lett.* **102**, 176807 (2009).

30. Supported by the Deutsche Forschungsgemeinschaft, the European Union (IP SCALA), EuroQUAM (L.H.), the Defense Advanced Research Projects Agency (Optical Lattice Emulator program), the Air Force Office of Scientific Research, the German-Israeli Project Cooperation (DIP) (E.A. and I.B.), the U.S.-Israel Binational Science Foundation (E.A. and E.D.), and MATCOR (S.W.).

Supporting Online Material
www.sciencemag.org/cgi/content/full/327/5973/1621/DC1
Materials and Methods
Figs. S1 and S2
References

11 November 2009; accepted 1 March 2010
10.1126/science.1184565

Strontium-Doped Perovskites Rival Platinum Catalysts for Treating NO_x in Simulated Diesel Exhaust

Chang Hwan Kim, Gongshin Qi, Kevin Dahlberg, Wei Li*

The high cost and poor thermal durability of current lean nitrogen oxides (NO_x) aftertreatment catalysts are two of the major barriers to widespread adoption of highly fuel-efficient diesel engines. We demonstrated the use of strontium-doped perovskite oxides as efficient platinum substitutes in diesel oxidation (DOC) and lean NO_x trap (LNT) catalysts. The lanthanum-based perovskite catalysts coated on monolith substrates showed excellent activities for the NO oxidation reaction, a critical step that demands heavy usage of platinum in a current diesel aftertreatment system. Under realistic conditions, $La_{1-x}Sr_xCoO_3$ catalysts achieved higher NO-to-NO_2 conversions than a commercial platinum-based DOC catalyst. Similarly, a $La_{0.9}Sr_{0.1}MnO_3$-based LNT catalyst achieved NO_x reduction performance comparable to that of a commercial platinum-based counterpart. The results show promise for a considerably lower-cost diesel exhaust treatment system.

There is a recognized need to lower greenhouse gas emissions from mobile sources in order to address concerns regarding global climate change. Diesel engines offer superior fuel efficiency and greenhouse gas reduction potential; however, one of the technical obstacles to their broad implementation is the requirement for a lean nitrogen oxide (NO_x) ($NO + NO_2$) aftertreatment system, a key contributor to the high cost premium for diesel vehicles. Unlike conventional gasoline engine exhaust, in which equal amounts of oxidants (O_2 and NO_x) and reductants (CO, H_2, and hydrocarbons) are available because of stoichiometric combustion, diesel engine exhaust contains excessive O_2 from combustion with much higher air-to-fuel ratios (>20). This oxygen-rich environment makes the removal of NO_x much more difficult. A typical diesel aftertreatment system includes a diesel oxidation catalyst, which oxidizes hydrocarbons, CO, and NO, followed by a NO_x reduction catalyst. Two of the most promising technologies for reducing NO_x under the oxygen-rich environment are ammonia selective catalytic reduction (SCR) and lean NO_x trap (LNT). In an SCR system, urea solution is injected into the diesel exhaust and decomposes to form ammonia, which then reacts selectively with NO_x to form N_2 and water. However, urea SCR systems require a secondary fluid tank with an injection system, resulting in added system complexity. Other concerns about urea SCR include urea infrastructure, the potential freezing of urea solution, and the need for drivers to periodically fill the urea solution reservoir. In an LNT-based aftertreatment system, the catalysts contain alkali or alkaline earth components (Ba, K, etc.) that store NO_x in the diesel exhaust to form metal nitrates and nitrites. Once the NO_x storage capacity in the LNT catalyst is saturated, the engine must run rich of stoichiometry (fuel-rich combustion) to generate excess reductants in the exhaust to remove the stored NO_x on the LNT catalysts and regenerate the NO_x storage capacity. However, the NO_x-absorbing components also react readily with sulfur oxides in the exhaust to form more stable metal sulfates, thus reducing the NO_x storage capacity. Treatment in a reducing environment at high temperatures (>650°C) is required to remove the S from LNT catalysts and recover the NO_x storage capacity.

Many reports have suggested that NO oxidation to NO_2 is an important step in lean NO_x reduction (*1*–*3*), because NO_2 enhances the activities of ammonia SCR and LNT. For SCR catalysts, a NO: NO_2 ratio of 1:1 is most effective for NO_x reduction at lower temperatures (<250°C). For LNT catalysts, NO must be oxidized to NO_2 before adsorption on the storage components. Because NO_2 constitutes less than 10% of NO_x in the diesel engine-out exhaust, an oxidation catalyst is required to increase the NO_2 fraction. Platinum has been found to be especially active for NO oxidation; thus, Pt-based diesel oxidation (DOC) and LNT catalysts have been widely used for diesel exhaust aftertreatment (*4*, *5*). However, they suffer from issues such as high cost and poor thermal durability. Consequently, there is substantial interest in the development of better-performing, low-cost, and more durable NO oxidation catalysts.

Here we report that perovskite catalysts show activities for NO oxidation similar to or higher than Pt-based commercial catalysts. Perovskite-based catalysts have been extensively investigated as potential substitutes for precious metal–based catalysts in automotive applications since the 1970s (*6*–*9*). The perovskite oxides have a general formula of ABO_3, where A designates a rare-earth or alkaline earth cation and B a transition metal cation (*9*). They are attractive because of their ease of synthesis, low cost, and high thermal stability (*10*, *11*). The La-based perovskite oxides (such as $LaCoO_3$, $LaMnO_3$, and $LaFeO_3$) have drawn particular interest because their catalytic properties can be easily tuned by substituting a

General Motors Global Research and Development, Chemical Sciences and Materials Systems Lab, 30500 Mound Road, Warren, MI 48090, USA.

*To whom correspondence should be addressed. E-mail: wei.1.li@gm.com

Downloaded from http://science.sciencemag.org/ on March 28, 2019

Science

Anomalous Expansion of Attractively Interacting Fermionic Atoms in an Optical Lattice

Lucia Hackermüller, Ulrich Schneider, Maria Moreno-Cardoner, Takuya Kitagawa, Thorsten Best, Sebastian Will, Eugene Demler, Ehud Altman, Immanuel Bloch and Belén Paredes

Science **327** (5973), 1621-1624.
DOI: 10.1126/science.1184565

Fermion Behavior in an Optical Lattice
Due to their extreme tunability, optical lattices loaded with fermions and bosons are expected to act as quantum simulators, answering complicated many-body physics questions beyond the reach of theory and computation. Some of these many-body states, such as the Mott insulator and the superfluid, have been achieved in bosonic optical lattices by simply changing the characteristic depth of the lattice potential wells. Now, **Hackermüller *et al.*** (p. 1621) describe an unusual effect in an optical lattice loaded with fermions: When the strength of the attraction between the fermions is increased adiabatically, instead of contracting, the gas expands in order to preserve entropy.

ARTICLE TOOLS	http://science.sciencemag.org/content/327/5973/1621
SUPPLEMENTARY MATERIALS	http://science.sciencemag.org/content/suppl/2010/03/24/327.5973.1621.DC1
REFERENCES	This article cites 25 articles, 1 of which you can access for free http://science.sciencemag.org/content/327/5973/1621#BIBL
PERMISSIONS	http://www.sciencemag.org/help/reprints-and-permissions

Use of this article is subject to the Terms of Service

Science (print ISSN 0036-8075; online ISSN 1095-9203) is published by the American Association for the Advancement of Science, 1200 New York Avenue NW, Washington, DC 20005. 2017 © The Authors, some rights reserved; exclusive licensee American Association for the Advancement of Science. No claim to original U.S. Government Works. The title *Science* is a registered trademark of AAAS.

Downloaded from http://science.sciencemag.org/ on March 28, 2019